www.maajournal.com

Mediterranean Archaeology and Archaeometry
Vol. 20, No 3, (2020), pp. 199-219
Open Access. Online & Print.

DOI: 10.5281/zenodo.4016084

NON-DESTRUCTIVE TEST INVESTIGATIONS ON THE DETERIORATION OF ROMAN MAUSOLEUM IN KARADAĞ CENTRAL ANATOLIA, TURKEY

Mehmet Bahadır Tosunlar*[1], Arife Deniz Oktaç Beycan[2] and Mustafa Korkanç[3,4]

[1]Muş Alparslan University, Department of Architecture, Turkey
[2]Konya Technical University, Department of Architecture, Turkey
[3]Niğde Ömer Halisdemir University, Department of Geological Engineering, Turkey
[4]Industrial Raw Materials and Building Materials Application and Research Center, Niğde Ömer Halisdemir University, Turkey

Received: 21/08/2020
Accepted: 20/09/2020
**Corresponding author: Mehmet Bahadır Tosunlar (bahadada@gmail.com)*

ABSTRACT

The Binbirkilise region has maintained its existence as an important religious and cultural center from the Hittites to the last period of the Eastern Roman Empire. There are many monuments in the region dating back to these periods. Among the region monuments, a Roman mausoleum draws attention along with its construction system and original form. This mausoleum was recently (2015) completely unearthed in the archaeological excavations carried out by the archaeologists of the Karaman Museum. Since then serious deterioration problems started to occur of atmospheric, biological and human origin. Several non destructive techniques (NDT) were applied and relevant measurements undertaken such as; temperature (ST), surface moisture (SM), Schmidt hammer rebound (SHR), and P-wave velocity (Vp) tests, 3D photogrammetry, thin sections, polarizing microscope, XRF analyses, XRD, mainly used to determine the deterioration conditions of building stones on the surface. The NDM innovative approach contributed to the understanding of the deterioration dynamics. It has been determined that a white crust formation on the parts of the monument unearthed by excavations and this crust formation affects the deterioration process of the building stones.

KEYWORDS: Roman mausoleum, deterioration, building stones, Non-destructive tests, archaeological excavations

1. INTRODUCTION

Excavations performed at archaeological sites are areas where the cultural heritage of humanity is discovered. For ancient stone monuments, the mechanisms of deterioration at archaeological sites differ in stones buried in the soil and unburied (Cronyn and Robinson, 1990; El-Gohary and Redwan, 2018; Kaplan et al., 2013) because building stones under and above the soil are affected by different deterioration factors.

Deterioration of building stones buried in the soil varies depending on soil temperature at different layers, soluble salts, dissolved carbon dioxide, organic matter content in the soil, pH value, vegetation cover, drainage conditions, hydrological status, climate, and soil structure (Cronyn and Robinson, 1990; Curran et al., 2002; Gauthier and Burke, 2011; Kaplan et al., 2013; Kibblewhite, 2015; Kibblewhite et al., 2015; Thorn et al., 2002; Velde and Meunier, 2008).

The main factors of deterioration in building stones, which always been on the surface are of atmospheric, biological, and anthropogenic origin. Deterioration phenomena due to atmospheric events are examined under the main headings of freeze-thaw (Fener and İnce, 2015; Gökçe et al., 2016; Ondrasina et al., 2002; Siegesmund et al., 2002; Freire-Lista et al., 2015), thermal shock (Wang et al., 2016; Bonazza et al., 2009; Paradise, 2000; Gomez-Heras et al., 2006), wetting-drying (Zhao et al., 2018; Zhou et al., 2017; Huggett, 2011; Hall and Hall, 1996; Goudie, 2016), and salt crystallization (Benavente et al., 2007; Ulusoy, 2007; Camuffo, 1995; Benavente et al., 1999; Özşen et al., 2017; Stück et al., 2018). Biological effects represent the direct and indirect contribution of plants, lichens, fungi, bacteria, and algae to the physical and chemical disintegration of rocks (Gaylarde et al., 2018; Cutler and Viles, 2010; Korkanç and Savran, 2015; Warscheid and Braams, 2000; Warscheid, 2000; Korkanç and Savran, 2010; Doehne and Price, 2010). Anthropogenic effects are the destruction caused by mechanical interventions to building stones and the wear caused by direct human contact (Paradise, 2000; Pope et al., 2002; Zakar and Eyüpgiller, 2015; Ashurst and Dimes, 1998).

Building stones, which had buried before the excavations and which always been on the surface, are affected by different deterioration factors. However there is no study in the literature comparing deterioration observed at these different levels by non-destructive tests (NDT). Present NDT studies are mainly used to determine the deterioration conditions of building stones on the surface.

The current studies have examined the deterioration of stones unearthed after excavations and the deterioration of stones always been on the surface comparatively by laboratory experiments (Curran et al., 2002; Thorn et al., 2002; Warke et al., 2010; Kaplan et al., 2013; El-Gohary and Redwan, 2018), or they have mainly focused on the deterioration of stone monuments and building stones always been on the surface (Hatır et al., 2019; İnce et al., 2018; Korkanç et al., 2018; Tosunlar et al., 2018; Elyamani and Roca, 2018; Moussa, 2019; Abdel-Aty, 2019; Zhang et al., 2019; Puy-Alquiza et al., 2019; Theodoridou and Török, 2019; Bozdağ et al., 2020; Korkanç et al., 2019; Hatır, 2020; Hatır et al., 2020; Dursun and Topal, 2019; Işık et al., 2020).

Non-destructive testing techniques are widely used to determine the deterioration factors affecting building stones. However, considering the changes of these factors according to macro and micro climatic conditions together with NDT maps provides an innovative approach to understand the deterioration dynamics.

In this study, the deterioration in the mausoleum structure, part of which had remained buried for approximately 1300 years were investigated. This Roman mausoleum is located in Karadağ, which was an important religious and cultural center from the Hittite Empire to the Eastern Roman Empire (Garstang, 1944; Turgut, 2013, 2015; Kurt, 2011, 2013; Ramsay and Bell, 1909; Yıldız, 2016). Karadağ is located within the borders of Karaman province (Fig. 1a, b). The region is also called Binbirkilise. The ancient ruins in the region are concentrated in Madenşehri village (Fig. 1c-g).

The mausoleum, which constitutes the subject of this study and a large part of which had remained buried under the soil since the 7th century AD (Ramsay and Bell, 1909), was completely unearthed in 2015 as a result of the archaeological excavation carried out by Karaman Museum (Bell, 2020; Konyalı, 1967; Eyice, 1971; Kurt, 2011; Yıldız, 2016) (Fig. 2a-j). The region where the Mausoleum structure is located is a region where religious structures of the Christian period are observed predominantly. The Roman mausoleum structure in the region is regarded as one of the rare buildings dating back to pre-Christian period. There are also no sign of repair in the mausoleum. With this condition, the mausoleum is a building that has preserved its originality from the time it was built, unlike other monuments in the region. This Mausoleum has remained standing entirely without the intervention of restoration is one of the few examples in Turkey and surrounding countries. These features of the structure provide opportunities for objective observation of the stone deterioration processes in the study area (Figs. 2-3).

It is observed that the decay factors in this monument are significantly active, especially in the sections, which had buried before the archaeological excavations. This section is covered with a white crust formation. The deterioration processes observed in the section covered by this white crust formation seriously threaten the conservation of the monument.

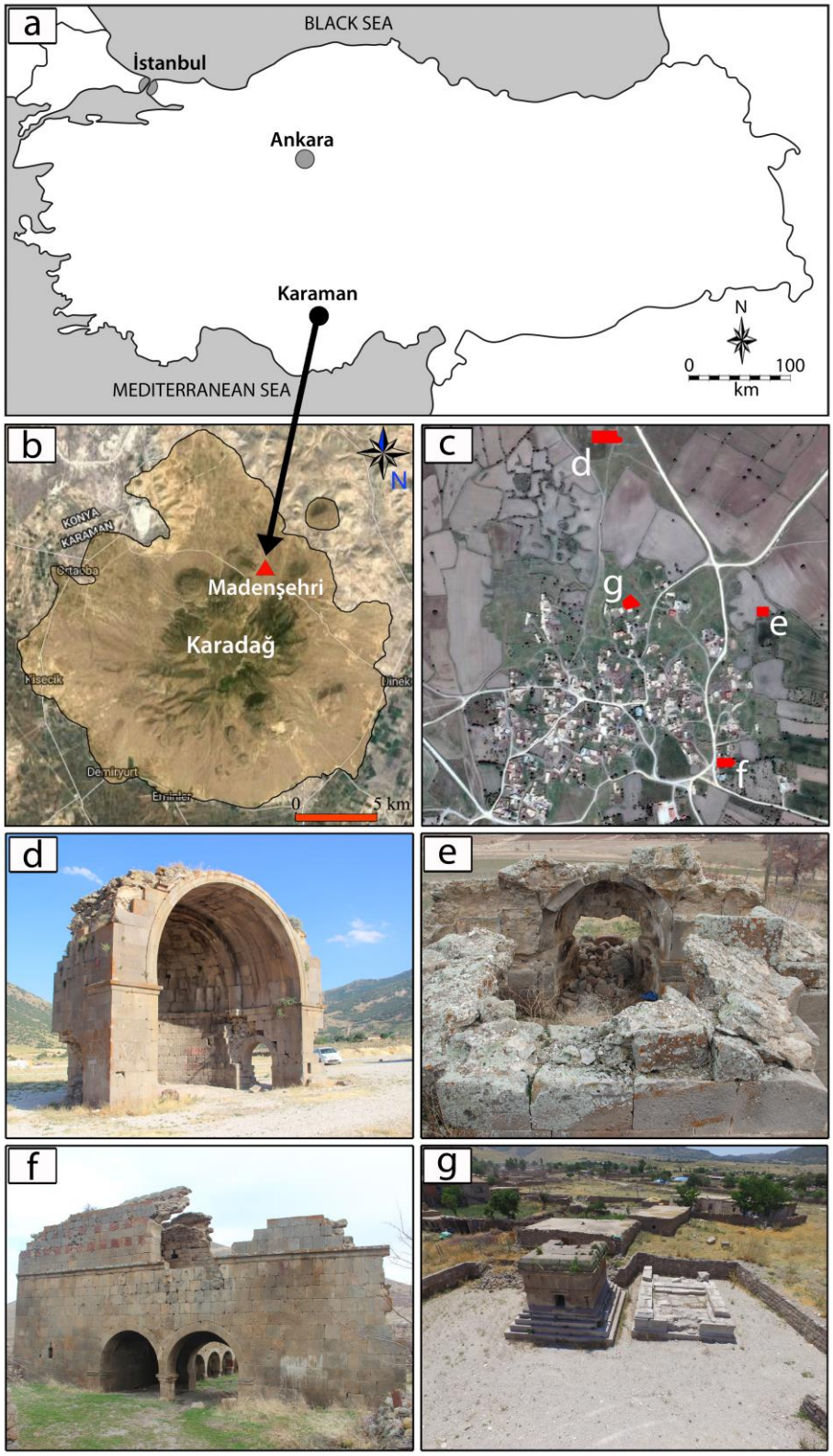

Figure 1. a) Location of Karaman Province, b) Location of Karadağ volcanism and Madenşehri village, c) Madenşehri village and important monuments, d) Exedra (4-5th centuries AD), e) Chapel No. 12 (early Byzantine period), f) Basilica No. 1 (5th century AD), g) Mausoleums (4-5th centuries AD).

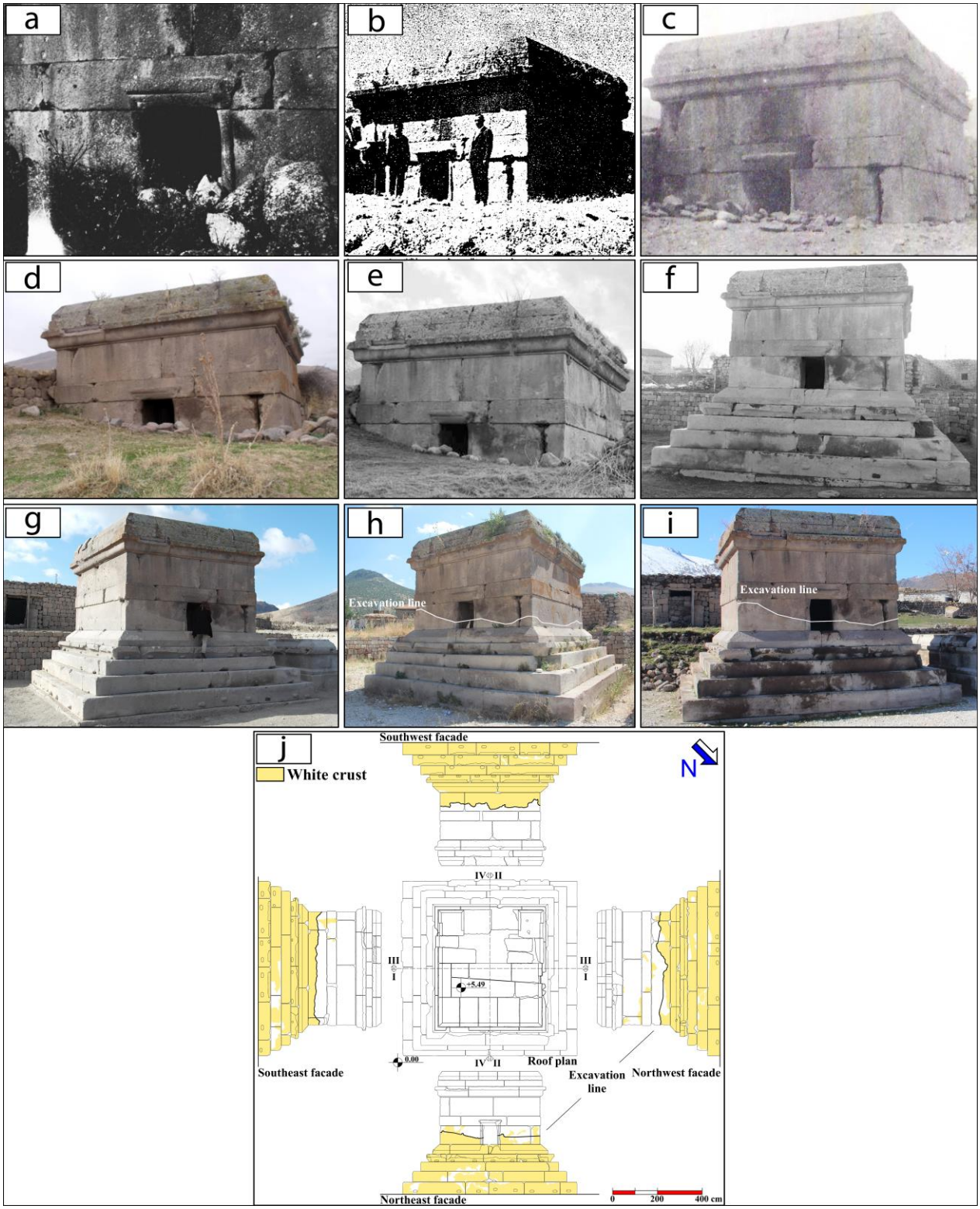

Figure 2. The pre-excavation and the post-excavation status of the mausoleum; a) 1907 (Bell, 2020), b) 1967 (Konyalı, 1967), c) 1971 (Eyice, 1971), d) 2011 (Kurt, 2011), e) 2016 (Yıldız, 2016), f) 2016 (Yıldız, 2016), g) 2017, h) 2018, i) 2019, j) excavation line and building stones covered by the white crust.

To determine the deterioration differences observed in the monument's building stones, which had buried before the excavations and which always been on the surface, studies were conducted in situ and in the laboratory. In laboratory studies, the index-mechanical, petrographic, and geochemical properties of the monument's building stones were determined. By carrying out in situ studies, first of all, the types of deterioration were determined. At the second stage, non-destructive test (NDT) meas-

urements (surface temperature (ST), surface moisture (SM), Schmidt hammer rebound (SHR), and P-wave velocity (Vp) tests) were applied to each building stone, and data maps were created according to the results obtained. At the final stage, the relationships between the deterioration types of the building stones, which had buried before the excavations and which always been on the surface, and the NDT maps were compared, and it was attempted to reveal the factors causing deterioration. As a result of the study, it has been determined that there is a white crust formation on the parts of the monument unearthed by excavations. It has been determined that this crust formation affects the deterioration process of the building stones. In this study, the effect of the white crust covering the surfaces of the building stones uncovered from the soil on the deterioration processes was tried to be understood. The study is also intended to be a guide for deterioration problems that may arise after excavations in other monuments in the region.

Figure 3. Facade and interior views and details of the mausoleum; a) northeast facade, b) northwest facade, c) southwest facade, d) southeast facade, e) projections called tenon, f) stylized plant figures, g) top cover, h) pedestals found at the corners of the southwest facade and missing top cover stones, i) entrance gate of the tomb, j) northeast wall, k) northwest wall, l) southwest wall, m) southeast wall, n) earth-filled ground, o) stone consoles and ceiling.

2. MATERIALS AND METHODS

2.1. History, Importance and Characteristic of the Monument

The mausoleum is located in the northern part of the settlement area of Madenşehri village (Fig. 1c). There is no inscription on the monument, and it is dated to the period between the 4th and 5th centuries AD (Ramsay and Bell, 1909; Kurt, 2011; Eyice, 1971). It is not known for whom the mausoleum was built. This monument, which was built using andesite block stones, is one of the unique examples of the Roman mausoleum architecture in Anatolia.

The mausoleum is located on a square-based podium with a size of 7.80 x 7.80 m, and the height of the structure is 5.49 m. The podium has five steps, and the first three steps are undecorated (Fig. 3a, b, c, d). In some of the podium stones, there are projections, called tenon (Adam, 2005), which are used to put stones in their places in the structure (Fig. 3e). The fourth step of the podium is concave and curved, while the fifth step has a trapezoidal prismatic form. There are stylized plant motifs at the corners of these steps (Fig. 3f). Over the podium, there is a body section formed by smooth rectangular andesite stones. Above the body section, there is a superstructure system rising as a series of three stones. The top cover is flat (Fig. 3g), and it is differentiated by two pedestals and missing stones on the southwest side (Fig. 3h).

The entrance gate of the mausoleum is in the northeast direction and located 2.23 m above the ground (Fig. 3i). The mausoleum chamber, which can be reached by passing through the gate, has a rectangular shape and a size of 2.88 x 3.42 m. The walls of the chamber were formed by smooth rectangular andesite stones (Fig. 3j, k, l, m). There is earth filling on the floor of the chamber (Fig. 3n). The superstructure of the mausoleum chamber was formed by placing stones on top of each other in the form of consoles (Fig. 3o). The height of the interior part of the mausoleum chamber is 2.87 m.

2.2. Geography, Location and Climate Properties of the Study Area

Madenşehri, which is located at the north-western foothills of Karadağ, has an elevation of 1218 m from sea level and is located in an area where terrestrial climate prevails. Summers in the region are hot and dry, and winters are cold and snowy. During the year, the minimum and maximum precipitation occur in August and December, respectively (Table 1). The highest and lowest average temperatures in the region were recorded in July and January, respectively (MGM, 2019). The dominant wind direction in the study area is from the northwest (Table 1) (Meteoblue, 2020). These regional climatic conditions have an impact on the deterioration processes of the building stones. In the winter period, the presence of water that causes saturation in the building stones freezes in micro cracks and pore, especially when the air temperature drops below 0 °C. This daily effect causes deterioration on the building stone surfaces. In addition, the prevailing winds in the region reduce the surface temperatures of the building stones and increase the rate of development of biological colonizations, especially in winter, on the northern facades of the buildings.

Table 1. Meteorological records of Karaman station for the period of 1951–2018 (MGM, 2019) and Madenşehri Village wind rose (Meteoblue, 2020).

Month	Temperature (°C)			Monthly total precipitation averages (kg/m²)
	Average	Minimum	Maximum	
January	0.5	-3.8	5.5	41.4
February	1.9	-2.7	7.3	34.7
March	6.3	0.5	12.5	37.0
April	11.5	5.0	18.2	36.1
May	16	8.8	23.2	36.5
June	20.2	12.4	27.7	22.4
July	23.4	15.2	31.1	4.3
August	22.9	14.6	31.0	3.9
September	18.7	10.3	27.1	7.5
October	12.9	5.7	20.6	28.0
November	6.9	1.1	13.6	33.4
December	2.5	-1.8	7.5	46.5

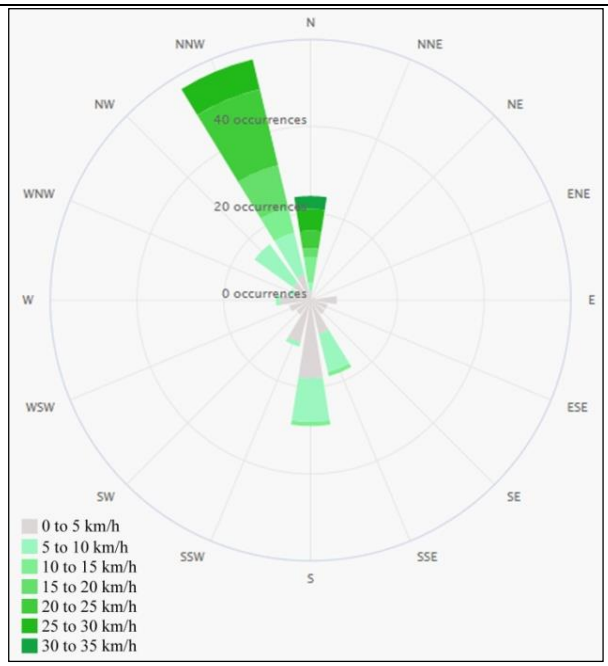

2.3. *Geology of the Study Area*

The study area is located in the Volcanic Region of Konya (Miocene-lower Pliocene), in the southern part of Central Anatolia (Sür, 1972). The part of these volcanites extending toward the east is called Karaman (Karadağ) volcanites (Ercan, 1986). In recent studies conducted in the study area, it has been stated that the Karadağ stratovolcano occurred in three stages and resulted in caldera collapse (Çoban et al., 2019). A non-parallel deep fault zone and other faults led to wide pull-apart basins, providing a pathway for volcanism, like the Karaman Basin, where the KS erupted in the region. The geological map of Karadağ and its surroundings is presented in Fig. 4. According to Gürsoy et al., (1998), Karaman (Karadağ) volcanites are Late Pliocene-aged.

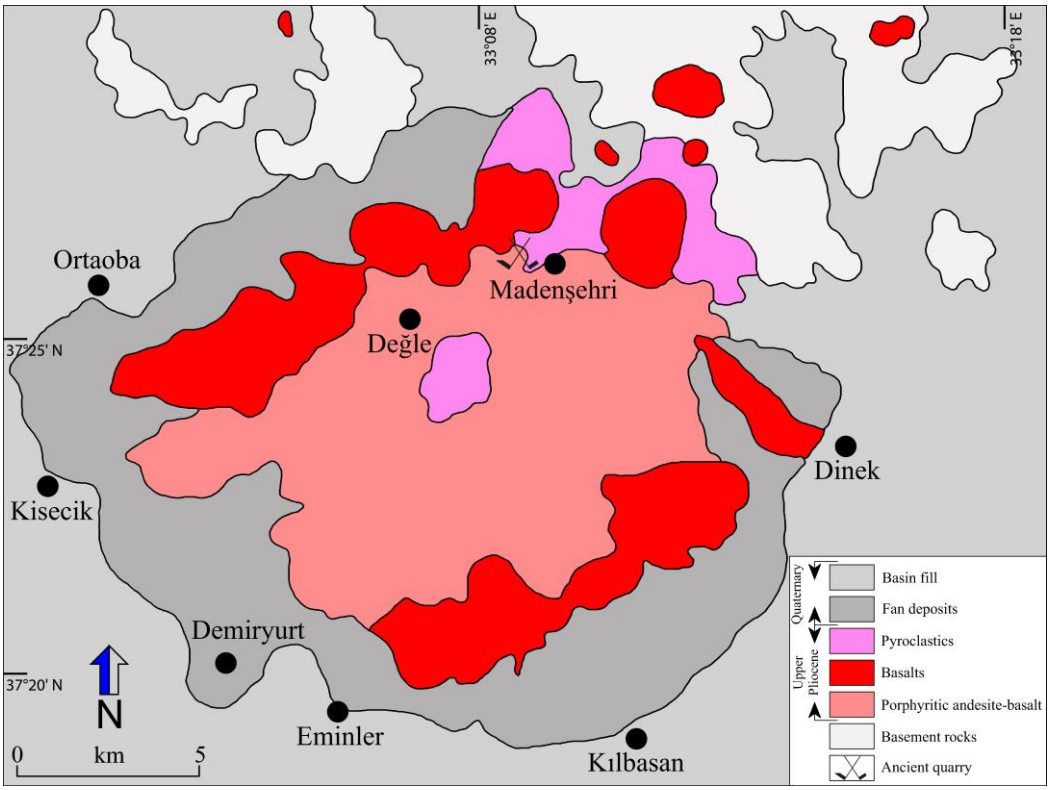

Figure 4. Geological units of Karadağ region and the location of the ancient quarry (Gürsoy et al., 1998).

2.4. *Methodology*

The experimental procedures of the study were carried out in three stages. These stages included observations of the monument and of the quarry samples, laboratory studies, and NDT measurements performed on the building stones.

2.4.1. Observations of the monument

The digital photogrammetry software was used to document the current status of the monument's facades and to map the deterioration of the building stones. The sequential photographs of the mausoleum taken at different locations and heights by a Canon 600D camera and DJI Phantom-3 Advanced air vehicle were processed in the Autodesk ReCap Photo program, and a 3D digital building model was obtained (Fig. 5a, b).

The scaled orthophotographs of each facade were taken from the 3D digital building model. These orthophotographs were evaluated together with the observations made in situ, and the scaled architectural plans and facade drawings of the building were prepared in the CAD environment (Fig. 5c). In the drawings, the deterioration types and the surface areas covered by them were mapped in detail. The deterioration types and their surface areas were measured and calculated from the 2D digital drawings, prepared in the CAD environment.

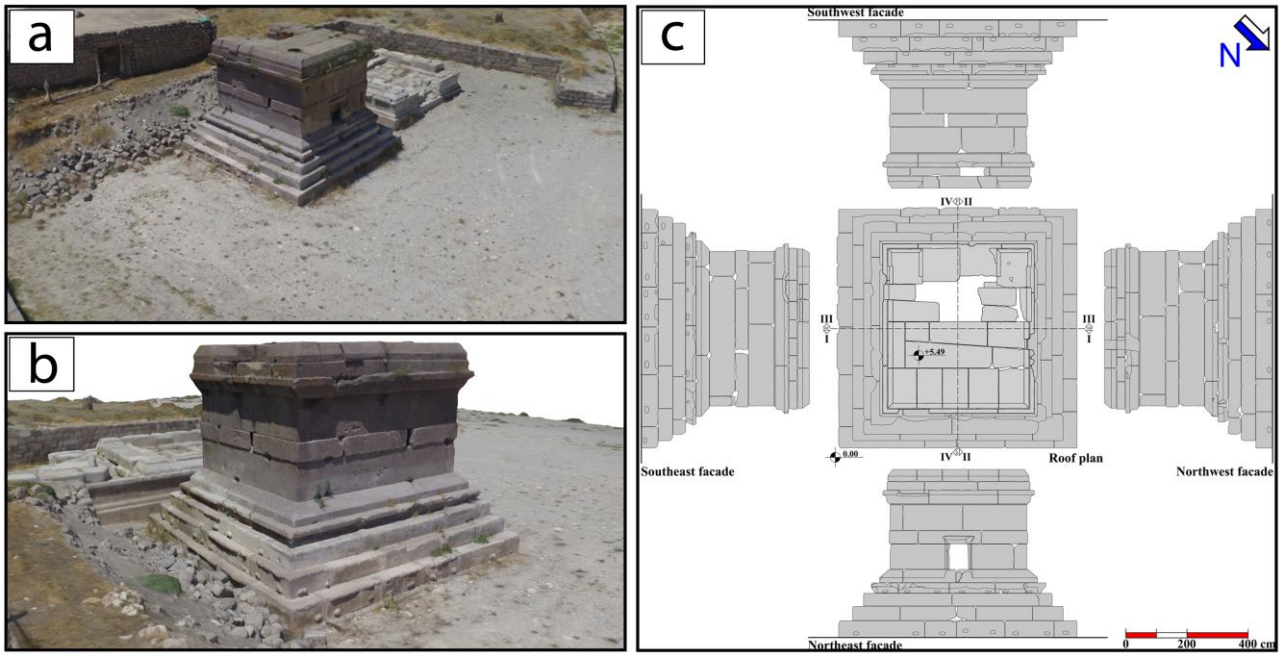

Figure 5. The modelling and drawing processes of the monument; a, b) scaled 3D model created in the Autodesk ReCap Photo program, c) scaled architectural plans and facade drawings prepared in the CAD environment.

2.4.2. Observations of the quarry samples

Due to conservation requirements, no stone samples were taken from the building, and samples were procured from the ancient quarry located north of Madenşehri village (Fig. 4). It is thought that this quarry was used until the 7th century AD after the settlement in the region ended (Ramsay and Bell, 1909). To determine the index - strength values of the building stones used in the monument before deterioration, fresh samples with colors, petrographic texture, and characteristics similar to the building stones were obtained from the ancient quarry. In the observations made in the quarry from which the stones used in the construction of the monument were taken, no white crust formation was found.

2.4.3. Laboratory Studies

From the andesite samples collected from the ancient quarry, samples were prepared in such a way that their size was NX (54 mm diameter) and their length was 2.0 - 2.5 times the width. The physical (dry density, porosity, water absorption by weight, capillary water absorption) and mechanical (SHR, Vp, and uniaxial compressive strength) properties of these samples were determined in accordance with the relevant standards and suggested methods (ASTM D5873, 2014; ISRM, 2007; TS EN 1925, 2000; ASTM D7012, 2014).

The thin sections, prepared to determine the petrographic properties of the rock samples, were examined under a polarizing microscope, according to TS EN 12407, (2013). XRF analyses performed to determine the major-element composition of the rock

were carried out in the YEBİM Laboratory of Ankara University according to the standards set by USGS for volcanic rocks (basalt, andesite) using a Spectro XLAB 2000 PEDXRF (400-W Rh end window tube and Si (Li) detector with a resolution of 148 eV (1000 cps Mn Kα) device.

It was observed that the thickness of the white crust that covered all the surfaces of the structure, which had buried before the excavations varied between 0.1 mm and 0.9 mm. The samples taken to determine the chemical composition of the white crust in these sections were taken from the podium sections of the monument. The XRD analysis conducted to determine the composition of the white crust was carried out in the YEBİM Laboratory of Ankara University using an "Inel Equinox 1000" device (CoKα radiation obtained at 30 kV and 30 Ma, 5–80° 2θ investigation range, 0.030 ° step).

2.4.4. NDT Measurements

Among the NDT methods, surface temperature (ST), surface moisture (SM), Schmidt hammer rebound (SHR), and P-wave velocity (Vp) tests were applied perpendicular to the building stones and perpendicular to the wall, color tones were formed according to the data obtained, and the data were mapped.

2.4.4.1. Surface Temperature (ST) Tests

The surface temperatures of the building stones were measured using a Trotec BP17 handheld infrared thermometer. The temperature range of the device is - 50 °C to + 380 °C, and the spectral accuracy is between 8 - 14 μm. The surface temperature measurements were carried out in the form of seasonal observations (twice, in July, which is the hottest month in the region, and in January, which is the coldest month) and three times during the day (at 10.00, 12.00, and 14.00). Measurements were made at five different points (stone corners and midpoint) on the surface of each stone facing the same direction. By taking the arithmetic mean of the data obtained, the seasonal surface temperature values of each building stone were acquired.

2.4.4.2. Surface Moisture (SM) Tests

The surface moisture values of the building stones were determined using a Trotec T660 handheld surface moisture meter. The accuracy range of this device, which is capable of measuring up to approximately 40 mm in depth of stone surface, is between 0-200 digits. Each digit represents a moisture value of 0.5%. The device can provide healthy values of environmental temperatures between - 20 °C and + 60 °C.

The surface moisture measurements on the monument were carried out simultaneously with the temperature measurements three times a day (at 10.00, 12.00, and 14.00) and at the same points of the building stones. The seasonal surface moisture value of each building stone was obtained by taking the arithmetic mean of the data obtained.

2.4.4.3. Schmidt Hammer Rebound (SHR) Tests

To determine the surface hardness of the building stones, a DRC-Geohammer "L" type Schmidt hammer with an impact energy of 0.735 Nm was used. The Schmidt hammer measurements were performed perpendicular to 10 different points and surfaces on the same surface, as specified in ASTM D5873, (2014). For each building stone, the mean of the ten values obtained was calculated. Values that differed by more than seven units were not taken into account while taking the mean. Afterward, the arithmetic mean of the remaining values was taken, and the SHR value of each building stone was obtained.

2.4.4.4. P-Wave Velocity (Vp) Tests

The Vp values of the building stones were measured using a UK 1401 ultrasonic tester. The device has two ceramic-tipped probes, one transmitter and one receiver, and is capable of conducting dry measurements without any contact liquid. The measurements were performed at three different points, on the surface of each stone facing the same direction, according to the principles and procedures specified in ISRM, (2007) by employing the indirect method. The arithmetic mean of the data obtained was taken, and the indirect P-wave velocity value of each stone surface was obtained.

3. RESULTS AND DISCUSSION

3.1. Observations of the monument

The deterioration observed in the monument were evaluated under three main headings (atmospheric, biological, and anthropogenic). The evaluations of deterioration was based on the studies carried out by ICOMOS-ISCS, (2008) and Fitzner and Heinrichs, (2004). The most common type of deterioration in the monument is the white crust (encrustation) formed in the parts of the structure, which had buried before the archaeological excavations (Fig. 2f-j and Figs. 6-7). The XRD analysis results of the samples taken from this layer are presented in Fig. 8e. When the XRD peaks were evaluated, the white crust was determined to consist of calcite, illite, and dolomite minerals.

Regarding the white crust formation process, several effects are thought to have developed together. The first of these effects; It is the accumulation of erosion products adhering to the stone surfaces in time,

especially in rainy periods, due to the frequent effects of seasonal wetting-drying cycles of the stones at the ground level of the building. The building is thought to have occurred in the form of stages towards the excavation line of the process of being covered. Rising soil accumulation is also thought to be effective in the formation of this crust by raising the wetting-drying line of the building stones (Fig. 7).

The second of the effects in the white crust formation process; It is the transport of minerals dissolved in the soil to the building stone surfaces with the water rising with the effect of capillarity. The soil minerals that are transported are deposited where they are transported by the effect of evaporation. It is thought that the raising soil accumulation in the past time creates a capillary effect at higher elevations and raises the crust formation to the excavation line. The calcite mineral determined by Özaytekin and Karakaplan, (2011) in the soil of the region and the content of the crust makes this effect possible.

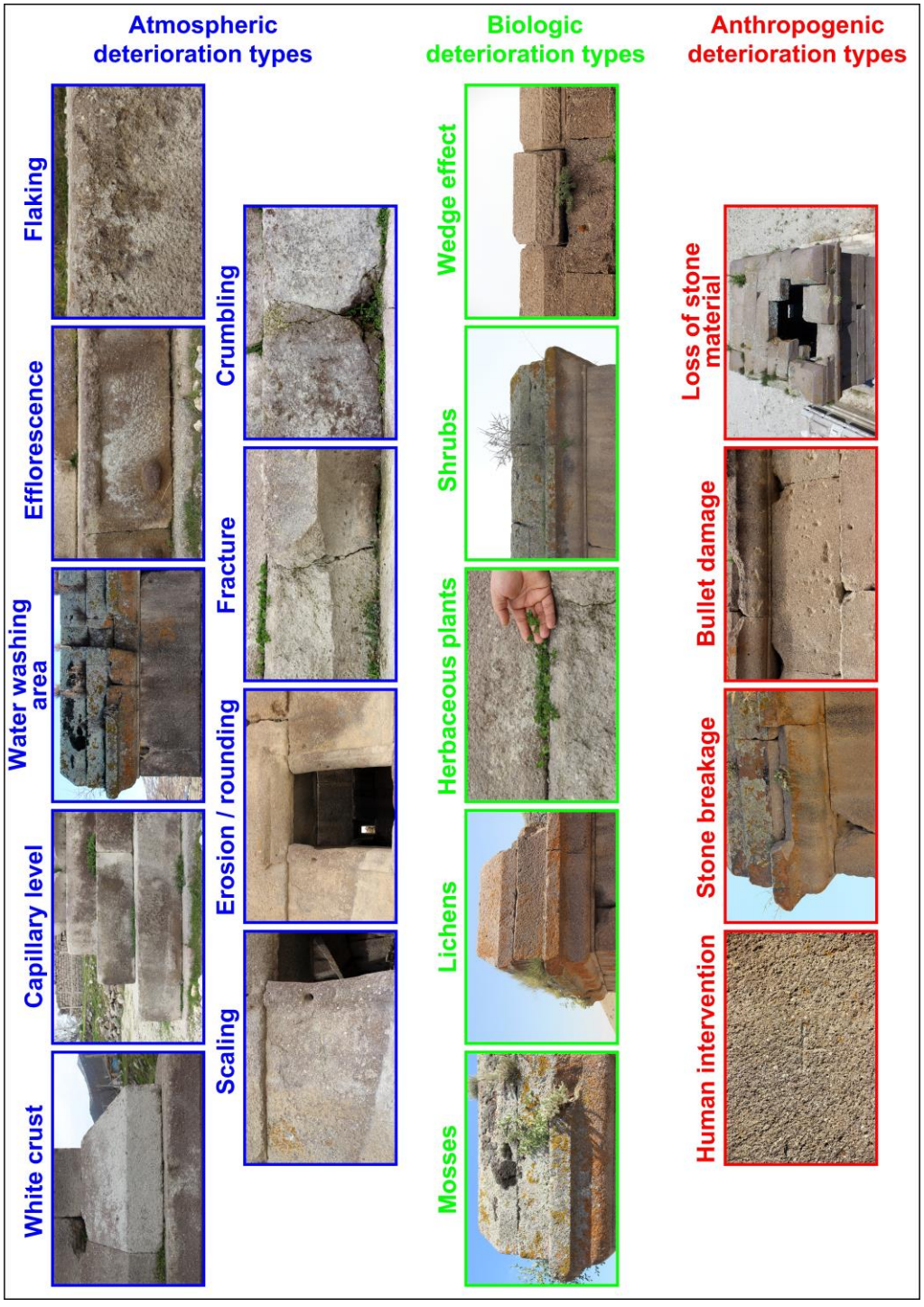

Figure 6. The main types of deterioration observed in the monument.

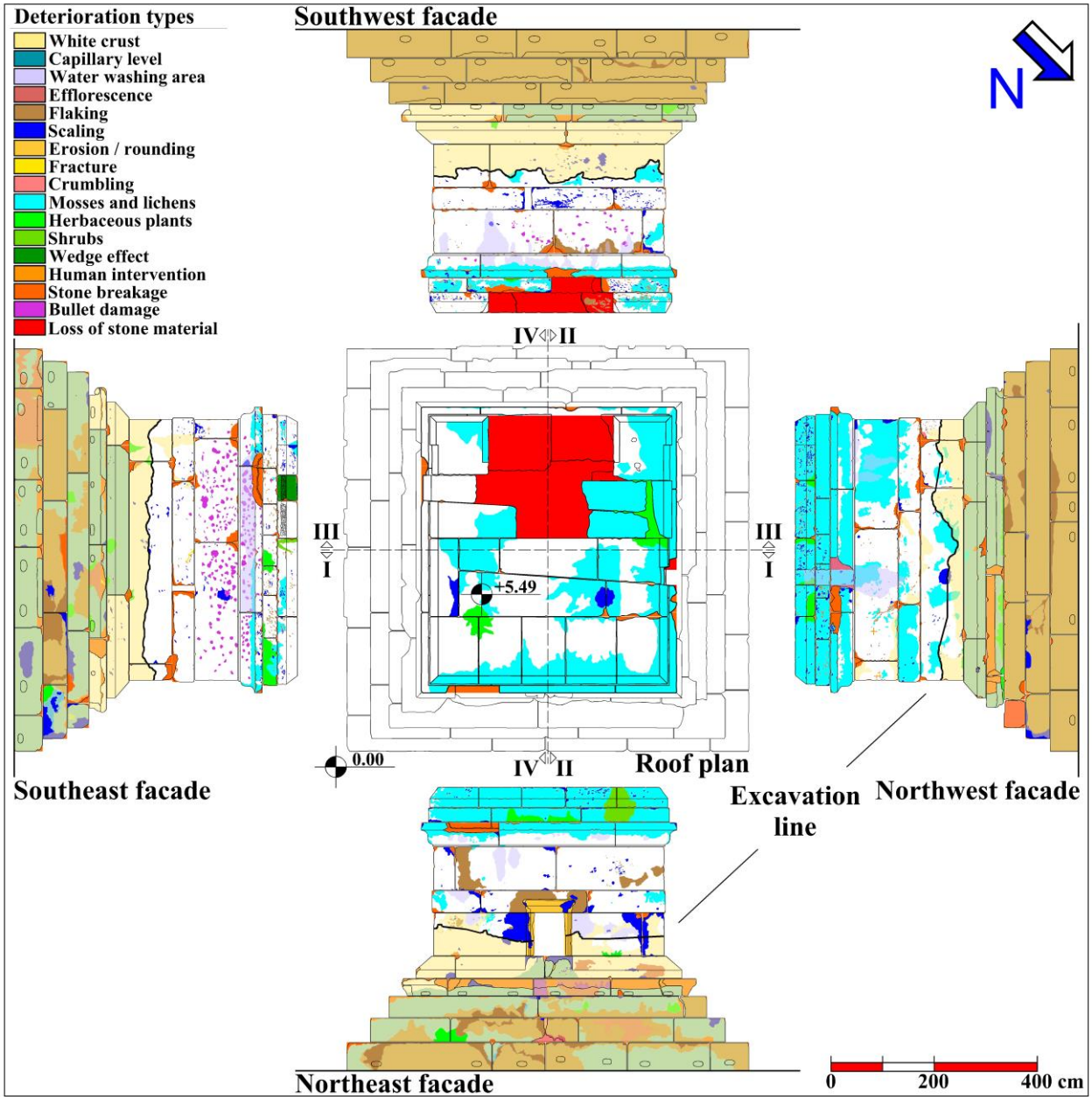

Figure 7. Map of the deterioration types in the mausoleum.

The decomposition process on the building stone surfaces is also effective in the formation of the white crust. The presence of illite, a change product of feldspar in the rock composition supports this effect (Fig. 8e).

The deterioration observed in the structure differs in the parts where it is covered and not covered by the white crust. In the section covered by the white crust, the most remarkable types of deterioration are of atmospheric origin (Table 2). It is calculated from the 2D digital drawings prepared in CAD environment where atmospheric deterioration types in this section cover 50.51% of the surface area. However in the section not covered by the white crust, the types of deterioration, which is atmospheric origin cover only 5.43% of the surface area (Table 2).

When the biological activities in the monument were examined, their strong relationships with the white crust were determined. While the rate of herbaceous plants was higher in the crust region (2.48%) with intense atmospheric deterioration, the biological activity layer consisting of algae and lichens was observed to be dominant in the parts, which always been on the surface (29.34%) (Table 2).

The development of herbaceous plants in the crust region was thought to be related to the high moisture due to the capillary effect and the soil remnants that could not be cleaned sufficiently during the excavation. The algae and lichen layer was concentrated to a large extent in the top cover region of the structure (Figs. 6-7). Herbaceous plants and shrubs that develop between the top cover stones together with this layer

cause the wedge effect between the building stones due to the growth forces formed by the roots (Figs. 6-7). As a result of these separations, the penetration of the surface water into the building structure and the mausoleum chamber becomes easier.

The deterioration of anthropogenic origin were observed more prominently in the parts of the structure always being on the surface (6.97%) (Table 2). The oldest one of these deterioration is the religious symbols that were engraved by visitors coming to the region on different facades of the monument (Fig. 6). Flaking is observed on the surfaces of the engraved symbols as a result of atmospheric effects.

Table 2. Deterioration rates on the building stone surfaces.

Main category	Deterioration type	Deterioration rate (%)			
		Excavated		Unburied	
Water affected area	Capillary level	79.55	79.55	0.00	6.96
	Water washing area	0.00		6.96	
Atmospheric deterioration	Efflorescence	2.89	50.51	0.00	5.43
	Flaking	44.26		2.43	
	Scaling	2.97		2.30	
	Erosion / rounding	0.16		0.65	
	Fracture	0.05		0.04	
	Crumbling	0.18		0.01	
Biological deterioration	Moses and lichens	0.87	3.35	29.34	31.56
	Herbaceous plants	2.48		1.17	
	Shrubs	0.00		0.68	
	Wedge effect	0.00		0.37	
Anthropogenic deterioration	Human intervention	0.00	5.40	0.02	6.97
	Stone breakage	4.80		3.38	
	Impact damage	0.00		0.98	
	Loss of stone material	0.60		2.59	

The other significant anthropogenic deterioration observed in this section is the breakage caused by impact effects in the joints and building stone corners due to vandalism and treasure hunting activities. Surface roughness increased in the regions where the breakage occurred, and flaking started to develop on these surfaces (Figs. 6-7).

In the parts of the monument always being on the surface, the most interesting form of deterioration of anthropogenic origin is the destruction caused by shooting with guns (0.98%) (Table 2). The bullet traces in these parts indicate that the monument was used as a shooting target (Figs. 6-7).

The losses of the stone material in the southwestern part of the monument's top cover were identified as the most critical anthropogenic effect damaging the building significantly (Figs. 6-7). The destruction of the stones in the roof cover causes precipitation to enter the mausoleum chamber easily. Precipitation entering these parts easily penetrates into the podium from the earth-filled ground. This infiltration is thought to accelerate the processes of decomposition by increasing the moisture content of the stones in the podium section.

The anthropogenic deterioration observed in the parts of the monument, which had buried before the archaeological excavations are stone breakages caused by possible impacts on the podium steps (4.80%) (Table 2). In addition, a step in the northern corner of this section has been completely destroyed (Fig. 7).

3.2. *Laboratory Studies*

Through the experiments conducted on the core samples, the average dry density (ρd) was found to be 1.98 g/cm³, porosity (n) 20.70%, water absorption (aw) 10.45%, and capillary water absorption (C) 337.20 $g/m^2s^{0.5}$. The average uniaxial compressive strength value (UCS) of the rock was found to be 54.20 MPa, the Schmidt hammer rebound (SHR) 46.20, and the P-wave velocity (Vp) 4015 m/s. According to the NBG, (1985) classification, the rock was in the "high porous rock" class and had the characteristics of "medium-strength" rock in terms of uniaxial compressive strength. According to De Beer, (1967), the rock was in the "very hard rock" class in terms of the SHR value.

In the thin section investigations of the sample under a polarizing microscope, which was procured from the ancient quarry and had a texture similar to the rock used in the building, 15% plagioclase, 18% clinopyroxene, 14% hornblende, 30% plagioclase microlites, 2% biotite, 2% opaque mineral, and 19% volcanic glass were determined (Fig. 8a, b, and c). The rock has typically a hyalopilitic texture.

The results obtained from the geochemical analysis of the rock sample are presented in Table 3. When the sample was assessed in the total alkali silica (TAS) diagram suggested by Le Bas et al., (1986), it was located in the andesite area (Fig. 8d).

Table 3. Major-element composition of the sample taken from the ancient quarry.

	Major oxide - %													
The sample of	SiO2	Al2O3	Fe2O3	MgO	CaO	Na2O	K2O	TiO2	P2O5	MnO	Cr2O3	SO3	V2O5	LOI
the ancient quarry	60.21	15.66	5.68	2.65	6.39	2.54	3.74	0.46	0.57	0.07	0.01	0.12	0.016	1.88

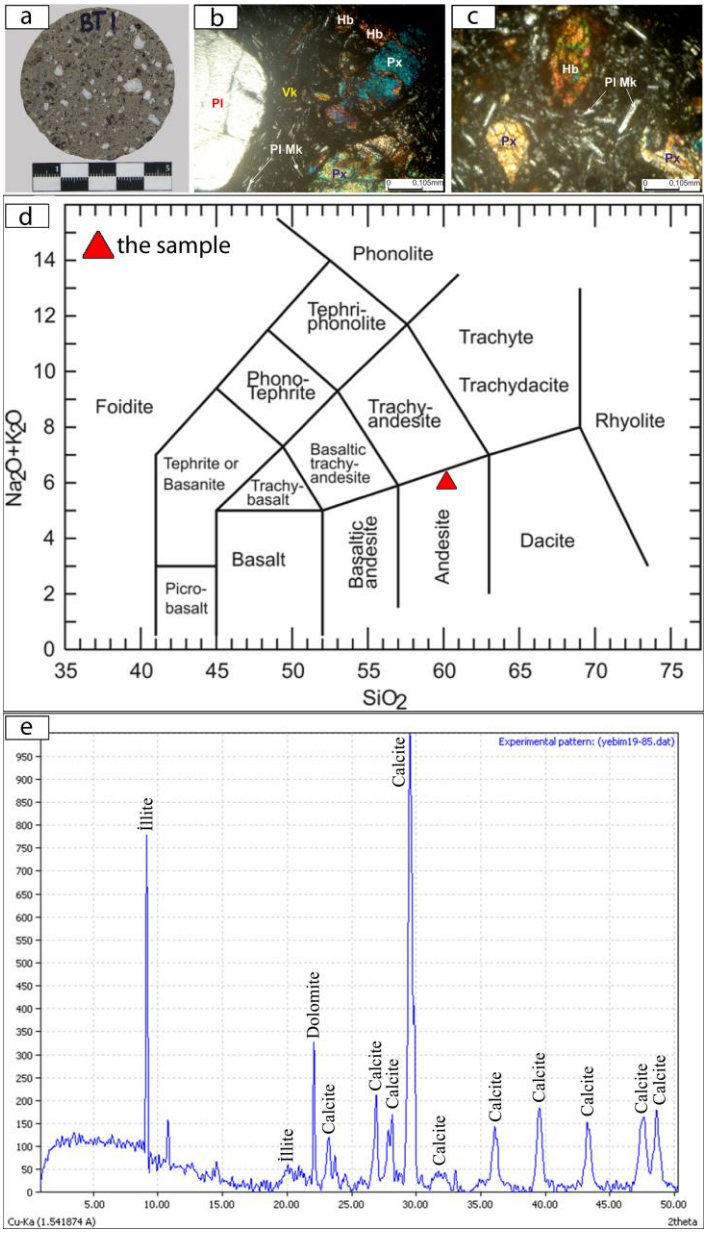

Figure 8. Macro and microscale photographs of the rock; a) macro view, b, c) thin section views (Pl: plagioclase, Vk: volcanic glass, Pl Mc: plagioclase microlites, Hb: hornblende, Px: clinopyroxene) (crossed nicols), d) assessment of the quarry sample in the TAS diagram Le Bas et al., (1986), e) XRD peaks of the white crust.

3.3. *NDT Measurements*

3.3.1. Surface Temperature (ST) and Surface Moisture (SM) Test Results

Daily and seasonal changes in temperature and moisture have a significant effect on the deterioration processes in building stones (Weiss et al., 2004; El-Gohary and Al-Shorman, 2010; Camuffo and Sturaro, 2001; Steiger et al., 2014; Huggett, 2011; Winkler, 1996; Warscheid and Braams, 2000; Mitchell et al., 2000; Tschegg, 2016; Smith et al., 2011; ANON, 1995). In this study, to determine the seasonal temperature and moisture changes in the mausoleum, measurements were carried out in summer and winter periods, and the results obtained were presented in Table 4 and Fig. 9.

Table 4. Seasonally measured ST and SM values in building stones.

NDT	Season	Location	Minimum	Maximum	Mean	(SD)
ST (°C)	Winter	Excavated	-9.7	17.8	2.63	7.65
		Unburied	-4.6	24.2	10.76	10.45
	Summer	Excavated	22.0	43.0	33.02	6.85
		Unburied	27.9	44.1	36.97	5.37
SM (%)	Winter	Excavated	52.0	100.0	85.50	10.72
		Unburied	32.0	92.0	67.54	14.40
	Summer	Excavated	19.0	75.0	44.77	10.21
		Unburied	15.0	56.0	35.33	10.49

Upon examining the values in Table 4, ST values of the sections always being on the surface are observed to be higher in summer and winter periods. However the building stones, which had buried before the archaeological excavations are colder. The reason for this is thought to be the archaeological remains covering the northwest part of the monument, high elevation slopes surrounding the monument, and the later built village house, as well as the change in the thermal and water permeability of the stones by the light-colored crust covering the surface.

In the winter period, ST falls below 0 °C in the majority of the building stones on the northwest facade. In the summer, the lowest temperatures were measured on this facade (Fig. 9a, b). Low temperatures on the northwestern facade of the monument can be explained by two main reasons. The first one is that the shadow caused by the archaeological remains close to the northwest facade and falling on this front restricts the period of sunlight exposure of the building stones. The second one is that the dominant wind direction in the region is from the northwest (Table 1). Due to the high elevation slopes and shading of the monument by the later built village house, low temperatures were also measured in the lower part of the southwest facade (Fig. 9a, b).

The highest average temperatures on the facades were measured on the southeast facade (Fig. 9a, b). This facade is a surface which the sun's rays can reach directly without any obstacle. The high temperatures on the facade create rapid evaporation, especially on stones in the podium section. Rapid evaporation reveals the problem of efflorescence.

Surface temperatures increase while moving toward the upper levels of the monument. Relatively lower temperatures were detected on the northeast and northwest facades of the top cover (Fig. 9a, b), where biological activity layers developed more.

The maximum SM values in the building stones were measured in the parts with the white crust (Table 4). High SM values in the lower part of the monument's podium during both summer and winter periods were associated with water rising from the soil by capillarity (Fig. 9c, d). High SM values observed in the steps of the upper part of the podium were thought to be caused by the seasonal precipitation waters leaking from the soil floor of the mausoleum chamber. High moisture that affects the building stones in the podium from both the ground and the upper part cannot evaporate due to the white crust covering the stone surfaces. This situation causes intense deterioration in the building stones under the effect of freeze-thaw cycles, especially in the winter periods. Increased the degree of saturation of rocks (increased humidity) causes the building stones to be more severely affected by freeze-thaw cycles as demonstrated in previous studies (Al-Omari et al., 2015; Chen et al., 2004; Prick, 1997; Matsuoka, 2001). This situation was also observed in building stone deterioration in this section. In addition the high moisture in this region also accelerates the growth of herbaceous plants.

The direct exposure of the building stones that make up the top cover of the monument to seasonal precipitations and the path which is followed by accumulated precipitation as it moves away from the structure constitute the infiltration zone (Figs. 6-7). High SM contents were determined in the stones in this zone, especially during rainy periods (Fig. 9d). High SM values in this region play an essential role in the occurrence of flaking and scaling on the building stone surfaces. High SM values also take a significant part in the development of biological formations in this section. The dominant winds from the northwest, which affect the building stones with a north-facing aspect, decrease temperatures and increase the development of mosses and lichens (Figs. 7-9).

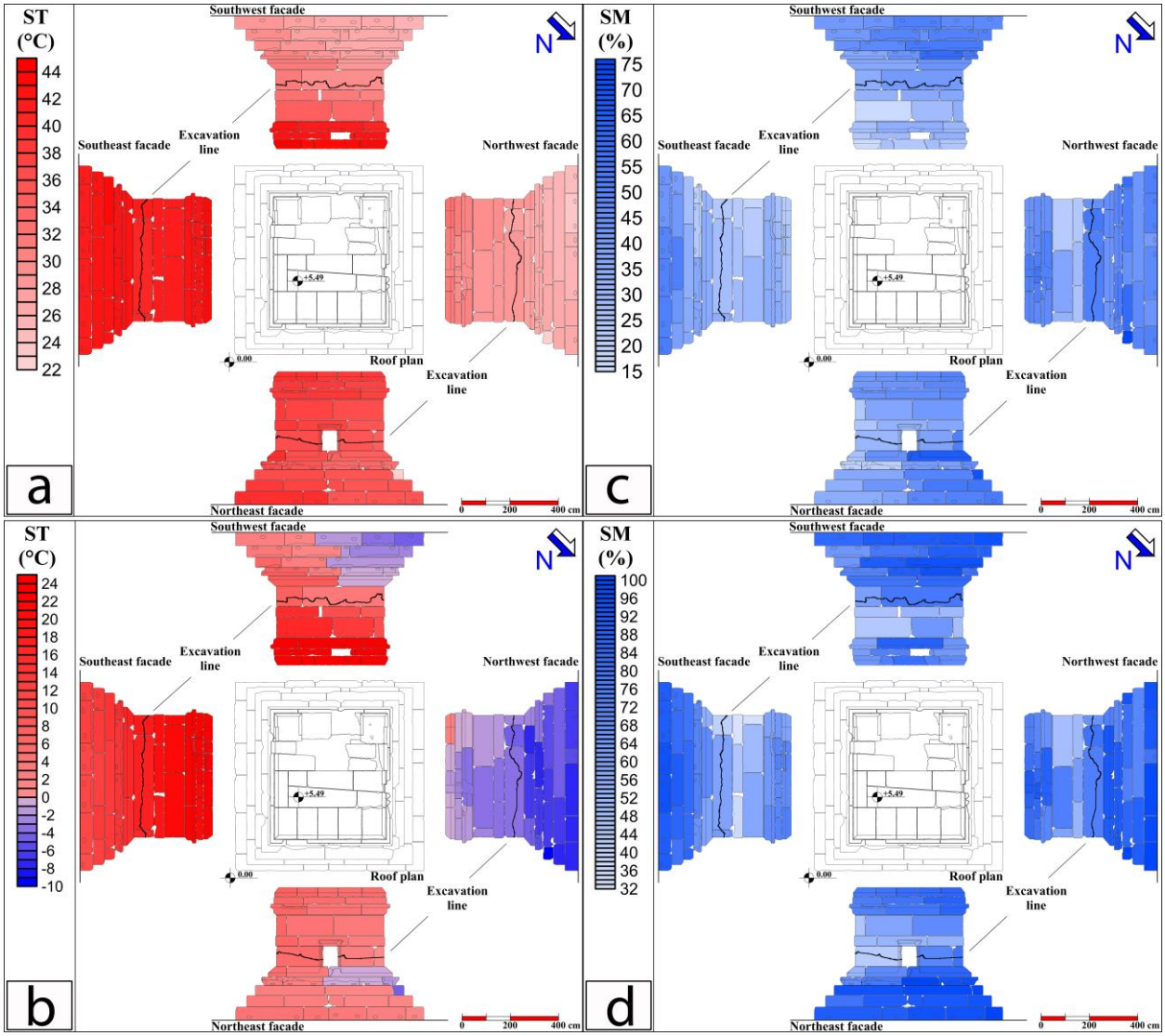

Figure 9. ST data maps of the monument; a) summer period, b) winter period, SM data maps of the monument; c) summer period, d) winter period.

3.3.2. Schmidt Hammer Rebound (SHR) and P-Wave Velocity (Vp) Test Results

To determine the deterioration effects in the building stones, Schmidt hammer rebound (SHR) and indirect P-wave velocity (Vp) measurements were performed on each building stone surface. The values obtained from the tests and the maps created depending on the values are presented in Table 5 and Fig. 10.

Upon examining the values in Table 5, it is observed that the SHR and Vp values are higher in the building stones always being on the surface throughout the history. This result indicates that although they were exposed to uninterrupted atmospheric effects, the building stones in this section suffered less deterioration than the building stones, which had buried before the archaeological excavations. When the SHR and Vp maps are examined, it is observed that the regions where these values are low are similar and that these regions are concentrated in the podium and roof parts (Fig. 10a, b). Furthermore, in the observations made in the regions where these two values were low, the deterioration was observed to be more intense.

Table 5. SHR and Vp values measured in building stones.

NDT	Location	Minimum	Maximum	Mean	(SD)
SHR	Excavated	13	35	24.94	4.30
	Unburied	13	41	26.56	6.71
Vp (m/s)	Excavated	1200	2900	2104.76	296.12
	Unburied	1300	3800	2459.77	544.84

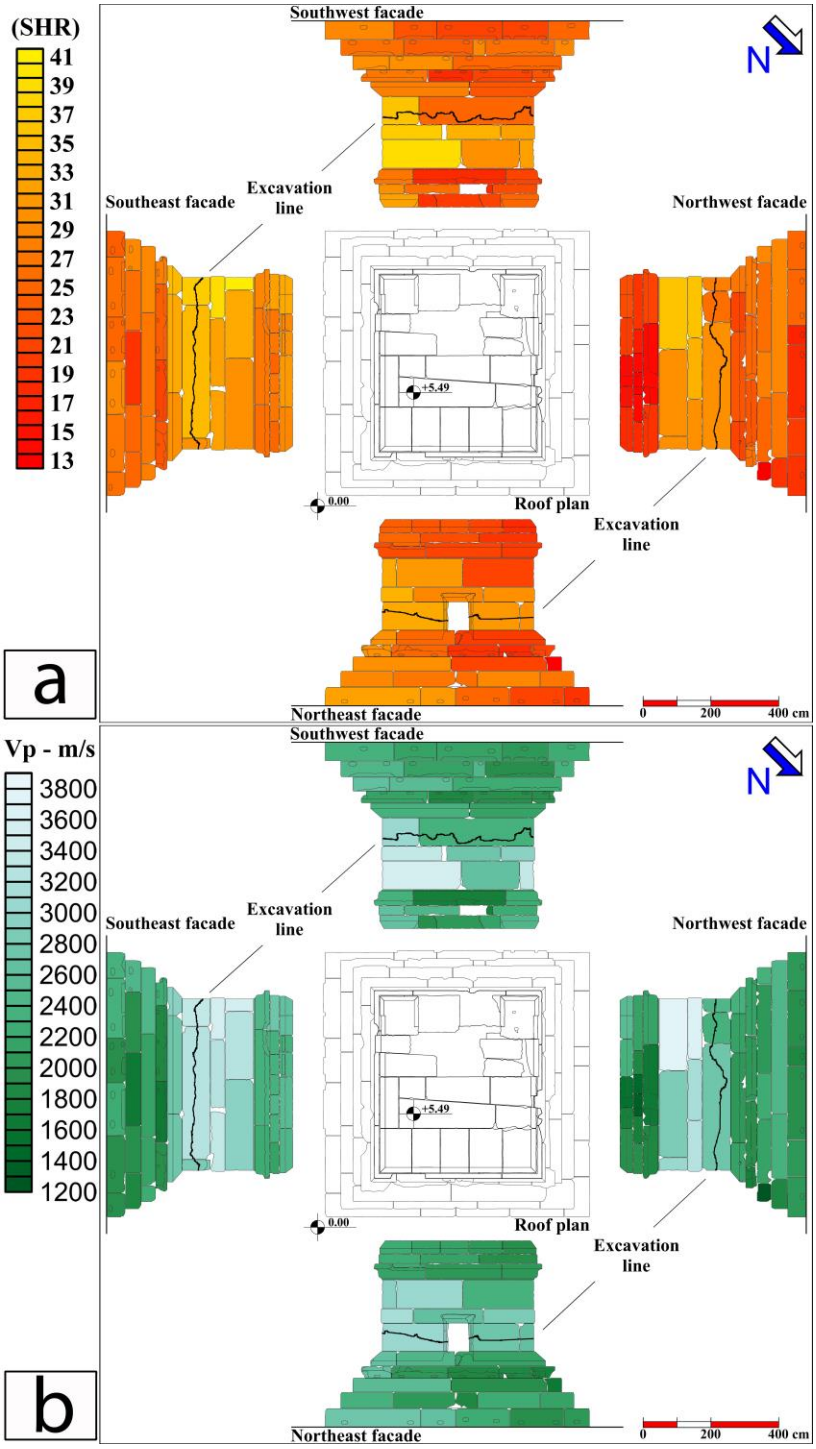

Figure 10. SHR and Vp data maps of the monument; a) SHR map, b) Vp map.

The low SHR and Vp values of the stones, always being on the surface, are associated with deterioration due to atmospheric effects and the intensive biological activity (mosses and lichens, herbaceous plants and shrubs). Furthermore, low SHR and Vp values were detected in the small-sized stones in this section. This can be explained by the fact that, as many researchers have noted (Yavuz, 2006; André et al., 2008; Korkanç, 2018; Tosunlar et al., 2018; Gökçe et al., 2016), as the sizes of building stones become smaller, the speed of their exposure to external factors increases, and the proportional size of microcracks formed during the shaping of small-sized building blocks increases (Fener and İnce, 2015).

In the part that had buried before the archaeological excavations, the deteriorated stones are concentrated on the ground and in the upper parts of the podium (Fig. 10a, b). At the same time, these sections constitute the regions with high SM values.

4. CONCLUSIONS

In this study, the unique mausoleum structure belonging to the Roman period and located in Madenşehri was investigated. It is thought that uncontrolled unearth of building stones without considering the microclimatic and environmental deterioration factors accelerates the processes of deterioration. Moreover, atmospheric effects changing from facade to facade, biological activities, and anthropogenic destruction constitute other important factors causing the deterioration of building stones.

The white crust prevents the evaporation of high humidity by covering the pores of the stones. Furthermore, the light color of the white crust causes temperatures in this section to decrease and the evaporation rate to slow down. High moisture content causes stones to be affected more by negative atmospheric effects, especially by freeze-thaw cycles.

The physical deterioration observed in the monument is compatible with the SHR and Vp maps. Moreover, significant correlations were also found between the ST and SM values measured in the summer and winter periods. Moisture values increase in the parts where temperature decreases. In addition, SHR and Vp values decrease in regions with increasing deterioration effects.

It was observed that the physical environment, which differed after the archaeological excavation, changed the microclimatic environment. It has been determined that the changing microclimatic environment especially increases the severity of atmospheric deterioration factors.

Present NDT studies are mainly used to determine the deterioration conditions of building stones on the surface. This study in which the building stones uncover from underground are compared with the building stones on the surface allowed the deterioration processes to be observed at different elevations within the monument.

REFERENCES

Abdel-Aty, Y. Y. A. (2019) Structural Evaluation of Façade Projections and Their Supporting Cambered Corbels at Historical Masonry Buildings in Cairo from Medieval Periods with a Proposal for Strengthening and Retrofitting. *Scientific Culture,* Vol. 5 (3), pp. 21-33.

Adam, J. P. (2005) *Roman Building: Materials and Techniques.* Routledge.

Al-Omari, A., Beck, K., Brunetaud, X., Török, Á. and Al-Mukhtar, M. (2015) Critical degree of saturation: A control factor of freeze–thaw damage of porous limestones at Castle of Chambord, France. *Engineering Geology,* Vol. 185, pp. 71-80.

André, M.-F., Etienne, S., Mercier, D., Vautier, F. and Voldoire, O. (2008) Assessment of sandstone deterioration at Ta Keo temple (Angkor): first results and future prospects. *Environmental Geology,* Vol. 56, pp. 677-688.

ANON (1995) The description and classification of weathered rocks for engineering purposes. *Quarterly Journal of Engineering Geology*, Vol. 28, pp. 207-242.

Ashurst, J. and Dimes, F. G. (1998) *Conservation of Building and Decorative Stone.* 2nd edition, Butterworth-Heinemann.

ASTM D5873 (2014) *Standard Test Method for Determination of Rock Hardness by Rebound Hammer Method*. ASTM International, West Conshohocken.

ASTM D7012 (2014) *Standard test methods for compressive strength and elastic moduli of intact rock core specimens under varying states of stress and temperatures*. Annual book of ASTM standards. American Society for Testing and Materials, West Conshohocken, pp 1–9.

Bell, G. (2020) Gertrude Bell Archive. http://gertrudebell.ncl.ac.uk/photo_details.php?photo_id=2177.

Benavente, D., Garcı□a del Cura, M. A., Fort, R. and Ordóñez, S. (1999) Thermodynamic modelling of changes induced by salt pressure crystallisation in porous media of stone. *Journal of Crystal Growth,* Vol. 204, pp. 168-178.

Benavente, D., Martínez-Martínez, J., Cueto, N. and García-del-Cura, M. A. (2007) Salt weathering in dual-porosity building dolostones. *Engineering Geology,* Vol. 94, pp. 215-226.

Bonazza, A., Sabbioni, C., Messina, P., Guaraldi, C. and De Nuntiis, P. (2009) Climate change impact: mapping thermal stress on Carrara marble in Europe. *Science of the Total Environment,* Vol. 407, pp. 4506-4512.

Bozdağ, A., İnce, İ., Bozdağ, A., Hatır, M. E., Tosunlar, M. B. and Korkanç, M. (2020) An assessment of deterioration in cultural heritage: the unique case of Eflatunpınar Hittite Water Monument in Konya, Turkey. *Bulletin of Engineering Geology and the Environment,* Vol. 79, pp. 1185–1197.

Camuffo, D. (1995) Physical weathering of stones. *The Science of the Total Environment,* Vol. 167, pp. 1-14.

Camuffo, D. and Sturaro, G. (2001) The climate of Rome and its action on monument decay. *Climate Research,* Vol. 16, pp. 145-155.

Chen, T. C., Yeung, M. R. and Mori, N. (2004) Effect of water saturation on deterioration of welded tuff due to freeze-thaw action. *Cold Regions Science and Technology*, Vol. 38, pp. 127-136.

Cronyn, J. M. and Robinson, W. S. (1990) *The Elements of Archaeological Conservation.* Routledge.

Curran, J., Smith, B. and Warke, P. (2002) Weathering of igneous rocks during shallow burial in an upland peat environment: observations from the Bronze Age Copney Stone Circle Complex, Northern Ireland. *Catena,* Vol. 49, pp. 139-155.

Cutler, N. and Viles, H. (2010) Eukaryotic Microorganisms and Stone Biodeterioration. *Geomicrobiology Journal,* Vol. 27, pp. 630-646.

Çoban, H., Karsli, O., Caran, S. and Yilmaz, K. (2019) What processes control the genesis of absarokite to shoshonite-banakite series in an intracontinental setting, as revealed by geochemical and Sr-Nd-Pb isotope data of Karadağ Stratovolcano in Central Anatolia, Turkey. *Lithos,* Vol. 324-325, pp. 609-625.

De Beer, J. (1967) Subjective Classification of the Hardness of Rocks and the Associated Shear Strength. *Proceedings of the 4th Reg Cong African Soil Mechanical Found Engineering.* Capctawn, pp. 396–398.

Doehne, E. and Price, C. A. (2010) *Stone Conservation: An Overview of Current Research*, Getty Publications.

Dursun, F. and Topal, T. (2019) Durability assessment of the basalts used in the Diyarbakır City Walls, Turkey. *Environmental Earth Sciences,* Vol. 78, pp. 456.

El-Gohary, M. A. and Al-Shorman, A. A. (2010) The impact of the climatic conditions on the decaying of Jordanian basalt at umm Qeis: exfoliation as a major deterioration symptom. *Mediterranean Archaeology and Archaeometry,* Vol. 10 (1), pp. 143-158.

El-Gohary, M. and Redwan, M. (2018) Alteration parameters affecting the Luxor Avenue of the Sphinxes-Egypt. *Science of the Total Environment,* Vol. 626, pp. 710-719.

Elyamani, A. and Roca, P. (2018) One Century of Studies for the Preservation of One of the Largest Cathedrals Worldwide: A Review. *Scientific Culture,* Vol. 4 (2), pp. 1-24.

Ercan, T. (1986) Cenozoic Volcanism of Central Anatolia. *Bulletin of the Mineral Research and Exploration,* Vol. 107, pp. 119-140.

Eyice, S. (1971) *Archaeological Investigations in Karadağ (Binbirkilise) and around Karaman.* İstanbul University Faculty of Letters Publications, İstanbul, in Turkish.

Fener, M. and İnce, İ. (2015) Effects of the freeze–thaw (F–T) cycle on the andesitic rocks (Sille-Konya/Turkey) used in construction building. *Journal of African Earth Sciences,* Vol. 109, pp. 96-106.

Fitzner, B. and Heinrichs, K. (2004) *Photo atlas of weathering forms on stone monuments.* Geological Institute, RWTH Aachen University Working group "Natural stones and weathering".

Freire-Lista, D. M., Fort, R. and Varas-Muriel, M. J. (2015) Freeze–thaw fracturing in building granites. *Cold Regions Science and Technology*, Vol. 113, pp. 40-51.

Garstang, J. (1944) The Hulaya River Land and Dadassas A Crucial Problem in Hittite Geography. *Journal of Near Eastern Studies,* Vol. 3 (1), pp. 14-37.

Gauthier, G. and Burke, A. L. (2011) The effects of surface weathering on the geochemical analysis of archaeological lithic samples using non-destructive polarized energy dispersive XRF. *Geoarchaeology,* Vol. 26 (2), pp. 269-291.

Gaylarde, C., Baptista-Neto, J. A., Tabasco-Novelo, C. and Ortega-Morales, O. (2018) Weathering of granitic gneiss: A geochemical and microbiological study in the polluted sub-tropical city of Rio de Janeiro. *Science of the Total Environment,* Vol. 644, pp. 1641-1647.

Gomez-Heras, M., Smith, B. J. and Fort, R. (2006) Surface temperature differences between minerals in crystalline rocks: Implications for granular disaggregation of granites through thermal fatigue. *Geomorphology,* Vol. 78, pp. 236-249.

Goudie, A. S. (2016) Quantification of rock control in geomorphology. *Earth-Science Reviews,* Vol. 159, pp. 374-387.

Gökçe, M. V., İnce İ., Fener, M., Taşkıran, T. and Kayabali, K. (2016) The effects of freeze–thaw (F–T) cycles on the Gödene travertine used in historical structures in Konya (Turkey). *Cold Regions Science and Technology*, Vol. 127, pp. 65-75.

Gürsoy, H., Piper, J. D. A., Tatar, O. and Mesci, L. (1998) Palaeomagnetic study of the Karaman and Karapinar volcanic complexes, central Turkey: neotectonic rotation in the south-central sector of the Anatolian Block. *Tectonophysics,* Vol. 299, pp. 191-211.

Hall, K. and Hall A. (1996) Weathering by wetting and drying: some experimental results. *Earth Surface Processes and Landforms,* Vol. 21, pp. 365-376.

Hatır, M. E. (2020) Determining the weathering classification of stone cultural heritage via the analytic hierarchy process and fuzzy inference system. *Journal of Cultural Heritage,* Vol. 44, pp. 120-134.

Hatır, M. E., Barstuğan, M. and İnce, İ. (2020) Deep learning-based weathering type recognition in historical stone monuments. *Journal of Cultural Heritage,* https://doi.org/10.1016/j.culher.2020.04.008 (İn press).

Hatır, M. E., Korkanç, M. and Başar, M. E. (2019) Evaluating the deterioration effects of building stones using NDT: the Küçükköy Church, Cappadocia Region, central Turkey. *Bulletin of Engineering Geology and the Environment,* Vol. 78, pp. 3465-3478.

Huggett, R. J. (2011) *Fundamentals of Geomorphology.* 3rd edition, Routledge.

İnce, İ., Bozdağ, A., Tosunlar, M. B., Hatır, M. E. and Korkanç, M. (2018) Determination of deterioration of the main facade of the Ferit Paşa Cistern by non-destructive techniques (Konya, Turkey). *Environmental Earth Sciences*, Vol. 77, (420).

ISRM (2007) *The complete ISRM suggested methods for rock characterization, testing and monitoring: 1974–2006*. In: Ulusay R., Hudson J. (eds) Suggested methods prepared by the commission on testing methods. ISRM Turkish National Group, Ankara, Turkey.

Işık, N., Halifeoğlu, F. M. and İpek, S. (2020) Nondestructive testing techniques to evaluate the structural damage of historical city walls. *Construction and Building Materials,* Vol. 253, pp. 119228.

Kaplan, Ç. D., Murtezaoğlu, F., İpekoğlu, B. and Böke, H. (2013) Weathering of andesite monuments in archaeological sites. *Journal of Cultural Heritage,* Vol. 14 (3), pp. e77-e83.

Kibblewhite, M., Tóth, G. and Hermann, T. (2015) Predicting the preservation of cultural artefacts and buried materials in soil. *Science of the Total Environment,* Vol. 529, pp. 249-263.

Kibblewhite, M. G. (2015) Predicting the Degradation of Buried Materials. *Proceedings of the Land Quality and Landscape Processes,* pp. 57- 61.

Konyalı, İ. H. (1967) *History of Karaman with its Monuments and Inscriptions, Ermenek and Mut Monuments.* Baha Printing House, İstanbul, in Turkish.

Korkanç, M. (2018) Characterization of building stones from the ancient Tyana aqueducts, Central Anatolia, Turkey: implications on the factors of deterioration processes. *Bulletin of Engineering Geology and the Environment,* Vol. 77, pp. 237-252.

Korkanç, M., Hüseyinca, M. Y., Hatır, M. E., Tosunlar, M. B., Bozdağ, A., Özen, L. and İnce, İ. (2019) Interpreting sulfated crusts on natural building stones using sulfur contour maps and infrared thermography. *Environmental Earth Sciences,* Vol. 78, pp. 378.

Korkanç, M., İnce, İ., Hatır, M. E. and Tosunlar, M. B. (2018) Historical Granaries at Taşkale (Turkey) Under Risk: A Geotechnical Analysis. *Mediterranean Archaeology & Archaeometry,* Vol. 18, pp. 149-162.

Korkanç, M. and Savran A. (2010) *Stones Used in Historical Buildings in Niğde Region and Their Problems*, TÜBİTAK Project, Project No: 106Y220, in Turkish.

Korkanç, M. and Savran, A. (2015) Impact of the surface roughness of stones used in historical buildings on biodeterioration. *Construction and Building Materials,* Vol. 80, pp. 279-294.

Kurt, M. (2011) Tombs of Binbir Kilise-Karaman. *Karamanoglu Mehmetbey University Journal of Social and Economic Research,* Vol. 13 (21), pp. 125-131, in Turkish.

Kurt, M. (2013) A Research Over The Hill of Karadağ-Mahalaç (Karaman). *Karamanoglu Mehmetbey University Journal of Social and Economic Research,* Vol. 15 (24), pp. 39-45, in Turkish.

Le Bas, M. J., Le Maitre, R. W., Streckeisen, A. and Zanettin, B. (1986) A chemical classification of volcanic rocks based on the total alkali-silica diagram. *Journal of petrology,* Vol. 27, pp. 745-750.

Matsuoka, N. (2001) Microgelivation versus macrogelivation: towards bridging the gap between laboratory and field frost weathering. *Permafrost and Periglacial Processes*, Vol. 12, pp. 299-313.

Meteoblue (2020) Windrose, Madenşehri, Turkey. https://www.meteoblue.com/en/weather/archive/windrose/maden%c5%9fehri_turkey_305022.

MGM (General Directorate of Meteorology) (2019) https://www.mgm.gov.tr/veridegerlendirme/il-ve-ilceler-istatistik.aspx?k=A&m=KARAMAN.

Mitchell, D. J., Halsey, D. P., Macnaughton, K. and Searle, D. E. (2000) The influence of building orientation on climate weathering cycles in Staffordshire, UK. *Proceedings of the 9th International Congress on Deterioration and Conservation of Stone,* pp. 357-365.

Moussa, A. (2019) Monitoring Building Materials Exposed to Marine Environment: Examples from Farasan Islands, Saudi Arabia. *Scientific Culture,* Vol. 5 (2), pp. 7-20.

NBG (1985) *Engineering Geology and Rock Engineering*. Norwegian Group of Rock Mechanics, Norway.
Ondrasina, J., Kirchner, D. and Siegesmund, S. (2002) Freeze-thaw cycles and their influence on marble deterioration: a long-term experiment. *Geological Society, London, Special Publications,* Vol. 205, pp. 9-18.
Özaytekin, H. H. and Karakaplan, S. (2011) Mineralogical Assessment of Soils Developed on Andesitic Materials at Mt. Karadag, Karaman from Central Anatolia. *Selçuk Journal of Agriculture and Food Sciences,* Vol. 25 (3), pp. 86-95.
Özşen, H., Bozdağ, A. and İnce, İ. (2017) Effect of salt crystallization on weathering of pyroclastic rocks from Cappadocia, Turkey. *Arabian Journal of Geosciences,* Vol. 10, pp. 258.
Paradise, T. R. (2000) Sandstone architectural deterioration in Petra, Jordan. *Proceedings of the 9th International Congress on Deterioration and Conservation of Stone*, pp. 145-154.
Pope, G. A., Meierding, T. C. and Paradise, T. R. (2002) Geomorphology's role in the study of weathering of cultural stone. *Geomorphology,* Vol. 47, pp. 211-225.
Prick, A. (1997) Critical Degree of Saturation as a Threshold Moisture Level in Frost Weathering of Limestones. *Permafrost and Periglacial Processes,* Vol. 8, pp. 91-99.
Puy-Alquiza, M. J., Ordaz Zubia, V. Y., Aviles, R. M. and Salazar-Hernández, M. D. C. (2019) Damage detection historical building using mapping method in music school of the University of Guanajuato, Mexico. *Mechanics of Advanced Materials and Structures,* pp. 1-12.
Ramsay, W. M. and Bell, G. L. (1909) *The Thousand and One Churches*. Hodder and Stoughton, London.
Siegesmund, S., Weiss, T. and Vollbrecht, A. (2002) Natural stone, weathering phenomena, conservation strategies and case studies: introduction. *Geological Society, London, Special Publications,* Vol. 205, pp. 1-7.
Smith, B. J., Srinivasan, S., Gomez-Heras, M., Basheer, P. A. M. and Viles, H. A. (2011) Near-surface temperature cycling of stone and its implications for scales of surface deterioration. *Geomorphology,* Vol. 130, pp. 76-82.
Steiger, M., Charola, A. E. and Sterflinger, K. (2014) *Chapter 4, Weathering and Deterioration*. Stone in Architecture Properties, Durability. 5th edition, Springer.
Stück, H. L., Platz, T., Müller, A. and Siegesmund, S. (2018) Natural stones of the Saale–Unstrut Region (Germany): petrography and weathering phenomena. *Environmental Earth Sciences,* Vol. 77, pp. 300.
Sür, Ö. (1972) *Geomorphological Research in the Volcanic Area of Turkey, Especially in Central Anatolia.* Ankara University publications, in Turkish.
Theodoridou, M. and Török, Á. (2019) In situ investigation of stone heritage sites for conservation purposes: a case study of the Székesfehérvár Ruin Garden in Hungary. *Progress in Earth and Planetary Science,* Vol. 6 (15), pp. 1-14.
Thorn, C. E., Darmody, R. G., Dixon, J. C. and Schlyter, A. P. (2002) Weathering rates of buried machine-polished rock disks, Kärkevagge, Swedish Lapland. *Earth Surface Processes and Landforms,* Vol. 27, pp. 831-845.
Tosunlar, M. B., Hatır, M. E., İnce, İ., Bozdağ, A. and Korkanç, M. (2018) The Determination of Deteriorations on the Mısırlıoğlu Bridge (Konya, Turkey) by Non-Destructive Techniques (NDT). *Iconarp International Journal of Architecture and Planning,* Vol. 6 (2), pp. 399-412.
TS EN 1925 (2000) *Natural stone test methods determination of water absorption coefficient by capillarity*. Turkish Standards Institution, Ankara, in Turkish.
TS EN 12407 (2013) *Natural stone test methods - Petrographic examination.* Turkish Standards Institution, Ankara, in Turkish.
Tschegg, E. K. (2016) Environmental influences on damage and destruction of the structure of marble. *International Journal of Rock Mechanics & Mining Sciences,* Vol. 89, pp. 250-258.
Turgut, M. (2013) *Reflections of the Hittite Mountain Cult, in Konya and the Vicinity of Karaman.* A Lifetime Dedicated to Historiography: Gift to Prof. Dr. Nejat Göyünç. pp. 559-574, in Turkish.
Turgut, M. (2015) Water Cult Spaces in Tarhuntašša. *The Pursuit of History, International Periodical for History and Social Research*, Vol. 14, pp. 337-354, in Turkish.
Ulusoy, M. (2007) Different igneous masonry blocks and salt crystal weathering rates in the architecture of historical city of Konya. *Building and Environment,* Vol. 42, pp. 3014-3024.
Velde, B. and Meunier, A. (2008) *The Origin of Clay Minerals in Soils and Weathered Rocks*. Springer.
ICOMOS-ISCS (2008) *ICOMOS International Scientific Committee for Stone (ISCS), Illustrated glossary on stone deterioration patterns.* Ateliers 30 Impression, Champigny/Marne, France.
Wang, P., Xu, J., Liu, S. Wang, H. and Liu, S. (2016) Static and dynamic mechanical properties of sedimentary rock after freeze-thaw or thermal shock weathering. *Engineering Geology,* Vol. 210, pp. 148-157.

Warke, P. A., Curran, J. M., Smith, B. J., Gardiner, M. and Foley, C. (2010) Post-excavation deterioration of the Copney Bronze Age Stone Circle Complex: A geomorphological perspective. *Geoarchaeology,* Vol. 25 (5), pp. 541-571.

Warscheid, T. (2000) *Integrated concepts for the protection of cultural artifacts against biodeterioration*. Of Microbes and Art, The Role of Microbial Communities in the Degradation and Protection of Cultural Heritage. Springer.

Warscheid, T. and Braams, J. (2000) Biodeterioration of stone: a review. *International Biodeterioration & Biodegradation,* Vol. 46, pp. 343-368.

Weiss, T., Siegesmund, S., Kirchner, D. and Sippel, J. (2004) Insolation weathering and hygric dilatation: two competitive factors in stone degradation. *Environmental Geology,* Vol. 46, pp. 402-413.

Winkler, E. M. (1996) Properties of marble as building veneer. *International Journal of Rock Mechanics and Mining Sciences and Geomechanics Abstracts,* Vol. 33, pp. 215-218.

Yavuz, A. B. (2006) Deterioration of the volcanic kerb and pavement stones in a humid environment in the city centre of Izmir, Turkey. *Environmental Geology,* Vol. 51, pp. 211-227.

Yıldız, A. (2016) Archaeological Excavations in Karaman, Binbir Kilise. *Proceedings of the 25. Museum Rescue Excavations Symposium and II. International Museology Workshop.* pp. 235–250, in Turkish.

Zakar, L. and Eyüpgiller, K. K. (2015) *Architectural Restoration Conservation Techniques and Methods.* Ömür Printing House, İstanbul, in Turkish.

Zhang, J., Huang, J., Liu, J., Jiang, S., Li, L. and Shao, M. (2019) Surface weathering characteristics and degree of Niche of Sakyamuni Entering Nirvana at Dazu Rock Carvings, China. *Bulletin of Engineering Geology and the Environment,* Vol. 78, pp. 3891–3899.

Zhao, Y., Ren, S., Jiang, D., Liu, R., Wu, J. and Jiang, X. (2018) Influence of wetting-drying cycles on the pore structure and mechanical properties of mudstone from Simian Mountain. *Construction and Building Materials,* Vol. 191, pp. 923-931.

Zhou, Z., Cai, X., Chen, L., Cao, W., Zhao, Y. and Xiong, C. (2017) Influence of cyclic wetting and drying on physical and dynamic compressive properties of sandstone. *Engineering Geology,* Vol. 220, pp. 1-12.